Desalination and Water Treatment
www.deswater.com

18 (2010) 61–70
June

1944-3994 / 1944-3986 © 2010 Desalination Publications. All rights reserved.
doi: 10.5004/dwt.2010.1317

Developing organic fouling indices of microfiltration and nanofiltration membranes for wastewater reclamation

Kangmin Chon[a], Sungyun Lee[a], Kyongmi Chon[a],
Ahamad Altaf Hussain[b], Jaeweon Cho[a,*]

[a]*Department of Environmental Science and Engineering, NOM National Research Laboratory (NRL),*
Gwangju Institute of Science and Technology (GIST), 261 Cheomdan-gwagiro, Buk-gu, Gwangju 500-712, Republic of Korea
Tel.: +82-62-970-2449; Fax: +82-62-970-2434; email: imonmyway@gist.ac.kr
[b]*Water Research and Development Center, Doosan Heavy Industries & Construction, Sh. Zayed Road, Office 6-112,*
Bldg. No. 6, Gold & Diamond Park, P.O. Box. 282350 Dubai, UAE
Tel.: +971-4-347-7051; Fax: +971-4-347-7142; email: altaf.hussain@doosan.com

Received 29 April 2009; Accepted 9 February 2010

ABSTRACT

Wastewater reclamation processes, including membrane bio reactor (MBR) and nanofiltration (NF) membrane, have been built, and those processes were independently operated, under recycling conditions, to compare the performances, with respect to contaminants removal and fouling minimization. The hydrophilic fractions of organic matter were more effectively removed than the hydrophobic fraction through the system due to microbial activities in the MBR, as measured using three dimensional fluorescence excitation and emission spectra. Furthermore, levels of nitrogen compounds, micropollutants, metals, and metalloid were substantially reduced by the applied MBR and NF system. These observations were in good agreements with patterns in molecular weight distributions and fluorescence spectra. The major components of membrane fouling in the system for wastewater reclamation were the hydrophilic fractions; high-performance size-exclusion chromatography, fluorescence and infrared spectra, and XAD 8/4 resins revealed that the hydrophilic fractions (non-humic substances), comprising of protein-like substances and saccharide groups, are responsible for serious membrane fouling in the tested system for wastewater reclamation.

Keywords: Wastewater reclamation; Fouling index; Membrane bio reactor; Nanofiltration

1. Introduction

Wastewater reclamation may be defined as a treatment process to provide reusable waters with reliable treatments that meet water quality criteria [1]. Some studies reported that role of membrane process for reclamation and reuse of municipal wastewaters [2–4], and most of previous studies have been conducted with main objectives of improvements of water qualities, in terms of chemical oxygen demand, turbidity, conductivity, and total hardness [5,6]. In addition, potential of membrane bio reactor (MBR) with nanofiltration (NF) membrane for wastewater treatment was evaluated [7–9], and its potential, with respects to removal of waterborne pathogens and nitrate, and disinfection by-products formation, were also examined [10].

Many studies have been focused on fouling control in the MBR process for wastewater reclamation [11,12]. However, membrane fouling mechanisms in wastewater reclamation system have not been well understood.

---

*Corresponding author.

Table 1
Membrane properties of MF in MBR system.

Membrane code	Type	Manufacturer	Materials	Pore size (μm)	Dimension (ID/OD) (mm)	Tensile strength (kg/fiber)
Cleanfil-S30V	MF	Kolon membrane Corporation	PVDF	0.1	0.8/2.0	>25

Membrane fouling which was formed through adsorption of organic matters, precipitation of inorganic species, and adhesion of microbial cells, at the surface of membrane, can cause continuous flux decline [13]. Thus, robust physical, chemical, and biological characterization should be performed to better understand and control membrane fouling in wastewater reclamation process.

Wastewater reclamation unit, including MBR and NF membrane, has been built to demonstrate its performances, with respect to contaminants removal and fouling minimization. Various parameters, such as specific ultraviolet absorbance (SUVA), and ratio of organic nitrogen to carbon (org-N/C), and many informative others, were employed as indicators to evaluate both performance and fouling formation, and structural analysis was also conducted to identify the relative hydrophobicity and hydrohpilicity for membrane foulants [14–16].

Research scope may include: (i) investigation of contaminants removal (in terms of organic matters, nitrogen compounds, metals, and metalloids) through the MBR–NF system; (ii) rigorous characterization of organic matters in raw wastewater, treated water, and membrane foulants (in terms of molecular weight (MW), functionality, and relative hydrophobicity, etc.); and (iii) development of organic fouling indices for quick and easy prediction/measurement of membrane fouling.

2. Materials and methods

2.1. System configuration and sample preparation

The MBR process was fed with municipal wastewaters (MBR feed), which were primary sedimentation effluents collected from the Gwangju wastewater treatment plant (WWTP) (Gwangju, Korea), and MBR effluent was further treated by NF membrane process to produce higher quality water. MBR and NF membrane processes were independently operated in recycling mode for one month to investigate removal efficiencies of contaminants and membrane foulants characteristics. Therefore, three different types of samples were collected to evaluate the performance of wastewater reclamation system: MBR feed, MBR effluent, and NF effluent. In addition, membrane foulants in MBR and NF membrane processes were chemically extracted with base (0.1 N NaOH) during 6 h, and then continuously extracted with acid (0.1 N HCl) during 6 h. The chemical and physical properties of the desorbed foulants were analyzed using various techniques, in terms of aromaticity, MW distribution, functionality, and relative polarity.

2.2. Operating conditions of MBR–NF systems

A laboratory scale wastewater reclamation system was comprised of one submerged type MBR and one NF membrane unit. A bioreactor, made of acrylic, with an effective volume of approximate 6.0 L, was filled with activated sludge which was provided from the Gwangju WWTP (Gwangju, Korea). In this wastewater reclamation system, the MBR was operated in a recycle mode in which permeate were returned to feed water reservoir, and a U-shaped hollow-fiber Polyvinylidene Fluoride (PVDF) microfiltration (MF) (Kolon, Korea) module was employed with an effective surface area of 150.7 cm^2. The properties of MF membrane are provided in Table 1. The hydraulic retention time (HRT) of MBR was 10 h and sludge retention time (SRT) was maintained at 10 days. Dissolved oxygen (DO) was continuously supplied by an air diffuser at an airflow rate of 2.5 L/min for complete mixing and microbial growth, and MBR effluents were taken out through the MF module using peristaltic pump at a flow rate of 10 ml/min. The operation conditions of MBR are listed in Table 2.

A typical bench–scale cross-flow membrane unit with the flat-sheet-type NF membrane was utilized for wastewater reclamation. The NF unit was operated

Table 2
Operating conditions of MBR process.

Bioreactor volume (L)	6.0
HRT (h)	10
SRT (d)	10
pH	6.66 ± 0.96
Conductivity (μS/cm)	656.7 ± 23.9
DO (mg/L)	9.43 ± 0.43
Temperature (°C)	18.0 ± 2.0

Table 3
Characteristics of NF membrane.

Membrane code	Type	Manufacturer	Materials	MWCO (Da)	Contact angle (°)	Zeta potential at pH 7(mV)	Roughness (nm)
NE90	NF (Tight)	Woongjin Chemical Corp.	Polyamide TFC	210	41.5	−36.4	34.3

also in a recycle mode in which both the retentate and permeate were returned to feed water reservoir. The effective area of NF membrane was approximate 58.2 cm^2. The NF membrane process was conducted at a room temperature (20 ± 2°C), and retentate flux was maintained at approximate 500 ml/min. Initial permeate flux was approximate 2.0 ml/min, but it decreased by 1.1 ml/min while initial permeate pressure of 517 kPa increased to 531 kPa. Membrane specifications of applied NF membrane are summarized in Table 3 [17].

2.3. Analytical methods

Dissolved organic carbon (DOC) concentration of samples was measured using a ultraviolet (UV)-oxidation-based total organic carbon (TOC) analyzer (TOC 800 analyzer, Sievers, USA). UV absorbance (UVA) at 254 nm of the samples was investigated by UV-visible spectrometer (UV-1601, Shimadzu, Japan). SUVA that is widely used to evaluate aromaticity of water samples was calculated from the ratio of UVA at 254 nm to DOC, and total nitrogen (TN) level was measured using a catalytic combustion type TOC analyzer equipped with nitrogen analyzer (TOC-V$_{CPH}$ with TNM-1 unit, Shimadzu, Japan). Moreover, anions (nitrite and nitrate) and cations (ammonium, calcium, and magnesium) were determined using ion chromatography (ICS-90, DX 120, Dionex, USA). Organic nitrogen (org-N) concentration was calculated using the following equation: org-N concentration = TN level − inorganic nitrogen level (i.e., nitrite, nitrate, and ammonium). The concentrations of metals and metalloid were measured by ICP–MS (7500ce, Agilent, USA), and the calibration curves were plotted using 10 μl/ml multi-element standard solutions (Agilent, USA). The target micropollutnants were extracted using solid phase extraction (AutoTrace automated SPE system, Claiper Corporation, Hopkington, MA, USA) and analyzed by liquid chromatography with Water 2695 Separations Module (Waters, Milford, MA, USA) coupled to a Micromass Quattro Micro triple-quadrupole mass spectrometer (Waters, Manchester, UK). A detailed procedure for analysis of pharmaceuticals was proposed [18]. High-performance size-exclusion chromatography (HPSEC) with Protein-Pak 125 column (Waters, Milford, MA, USA), UVA (SPD-10A$_{VP}$, Shimadzu, Japan), and fluorescence detections (RF-10A$_{XL}$, Shimadzu, Japan), was performed to ascertain MW distribution of aromatic and protein-like substances. The relationship between retention time and MW was derived with polystyrene sulfonates (MW of 210, 1.8, 4.6, 8, 18 kDa) [19]. The major components and complexity of membrane foulants were identified using fluorescence spectrophotometer (F-2500, Hitachi, Japan) that provides three dimensional fluorescence excitation and emission (3D FEEM) spectra by collecting the excitation and emission wavelength range from 220 to 500 nm. The freeze dryer (Ilshin, Korea) was utilized to make water samples powders, and infrared (IR) spectra with a KBr pellet (Pike, USA) were obtained using fourier transform infrared spectrometer (FT/IR–460 plus, Jasco, Japan) by collecting wave numbers in the range of 4000 cm^{-1}~700 cm^{-1}. Structural analysis using XAD–8/4 resins was conducted to determine relative hydrophobicity and hydrophilicity of organic foulants. Organics were fractionated into hydrophobic (adsorptive to XAD–8), transphilic (adsorptive to XAD–4) and hydrophilic fractions (neither adsorptive XAD–8 nor XAD–4) [20].

3. Results and discussion

3.1. Performance of the MBR–NF systems

Changes of water qualities, nitrogen compounds, metals, and metalloid by the wastewater reclamation system are summarized in Table 4. The water qualities, in terms of pH, conductivity, DOC level, UV absorbance, and SUVA are monitored. The pH slightly decreased through MBR process from nitrification which can consume alkalinity of the water [21], and conductivity was efficiently removed using NF membrane process. DOC concentration was significantly reduced by the MBR and NF membrane systems. DOC decreased, meanwhile, SUVA value substantially increased for the MBR–NF systems, meaning that hydrophilic fractions of organics were preferentially removed by the system [22]. In case of nitrogen compounds, ammonium ions were dominant nitrogen compounds in MBR feed water however ammonium ions were primarily oxidized into nitrate ions by nitrifying bacteria in MBR. Furthermore,

Table 4
Variations in water qualities, nitrogen compounds, metals and metalloids by MBR–NF systems.

		MBR feed	MBR effluent	NF effluent
Water qualities	pH	7.2 (±0.1)	6.4 (±0.9)	6.2 (±0.2)
	Conductivity (μS/cm)	771 (±5.5)	638 (±24.0)	69 (±3.1)
	DOC (mg C/L)	10.4 (±0.00)	4.3 (±0.28)	0.3 (±0.08)
	UV_{254} (cm^{-1})	0.129 (±0.0002)	0.119 (±0.0083)	0.017 (±0.0027)
	SUVA (L m^{-1} mg^{-1})	1.2 (±0.00)	2.8 (±0.07)	5.2 (±1.22)
Nitrogen compounds	Nitrite (mgN/L)	ND	10.5 (±8.9)	3.2 (±1.4)
	Nitrate (mgN/L)	ND	103.9 (±14.9)	17.4 (±2.6)
	Ammonium (mgN/L)	56.7 (± 0.9)	8.0 (±7.5)	2.2 (±0.5)
Metals and metalloid	Mg (mg/L)	7.50 (±0.25)	7.80 (±0.08)	0.21 (±0.01)
	Ca (mg/L)	26.12 (±0.34)	26.95 (±0.43)	0.91 (±0.10)
	Co (μg/L)	0.19 (±0.01)	0.15 (±0.03)	0.01 (±0.01)
	Cr (μg/L)	0.21 (±0.01)	0.19 (±0.04)	0.03 (±0.01)
	Fe (μg/L)	55.96 (±0.18)	11.98 (±2.20)	0.45 (±0.14)
	Mn (μg/L)	72.68 (±0.50)	10.66 (±8.35)	0.23 (±0.11)
	As (μg/L)	1.52 (±0.11)	1.99 (±0.11)	0.10 (±0.02)

ND: not detected.

it was confirmed that concentration of nitrate ions could be substantially removed by the NF membrane as NF membrane has a negatively charged surface at a neutral pH [23]. Through the MBR–NF systems, most metals, with the exception of calcium and magnesium, were efficiently removed by MBR while NF membrane could sufficiently reduce the concentration of most metals. However, removal efficiency of arsenic was lower than other metals, as an arsenite has a neutral charge at pH range of 4.5–8.5 (i.e., H_3AsO_3) [24].

Among the various micropollutants which are listed in Table 5, caffeine, naproxen, ibuprofen, and acetaminophen were substantially transformed or degraded by microbes present in MBR but other micropollutants were poorly degraded or transformed. Recent studies reported that caffeine, naproxen, ibuprofen, and acetaminophen were effectively controlled in MBR, and the micropollutants removal was influenced by sludge retention time (SRT) [25,26]. As expected, most micropollutants were effectively removed by the NF membrane.

Table 5
Micropollutants removal by wastewater reclamation system.

	MBR feed (ng/L)	MBR effluent (ng/L)	NF effluent (ng/L)
Atenolol	508	692	30
Caffeine	6158	74	13
Amlodipine	42	16	22
Sulfamethoxazole	166	170	10
Carbamazepine	86	98	ND
Glimepride	36	30	15
Clopidogel	18	14	4
Tris (2-carboxyethyl) phosphine (TCEP) TCEP	246	1056	344
Naproxen	2470	438	ND
Diclofenac	366	346	8
Ibuprofen	2114	1006	ND
Atetaminophen	2474	200	116
Iopromide	1852	1802	37

ND: not detected.

Fig. 1 exhibits variations in MW distribution of aromatic substances through the tested processes. The MW distribution with UV detection is comprised of both small (150, 310, 360, and 640 Da) and large (37,800 Da) portion of organics. The highest peak of aromatic substances corresponds to a peak at 360 Da. The changes

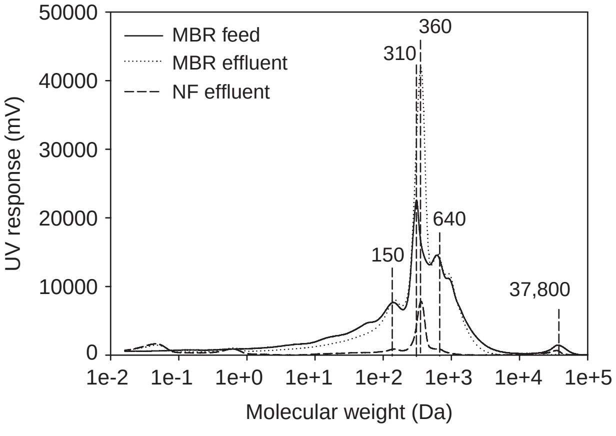

Fig. 1. Variations in MW distribution of aromatic substances through MBR–NF systems.

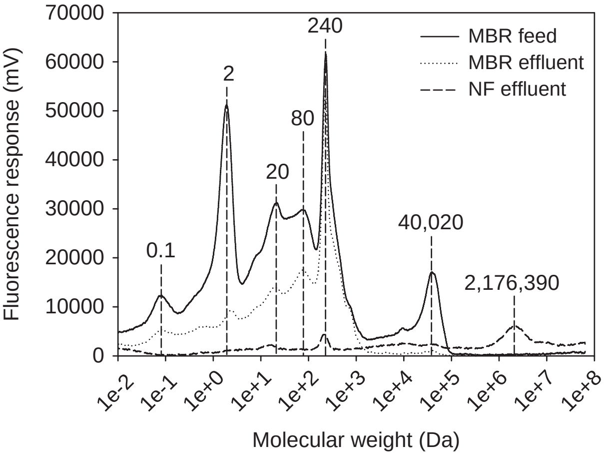

Fig. 2. Changes in MW distribution of protein-like substances through MBR–NF systems.

in MW distribution of protein-like substances through MBR–NF systems were represented in Fig. 2. The fluorescence response ranged from 0.1 to 2,176,390 Da, with the highest response at 240 Da. From the variations in MW distribution of aromatic and protein-like substances, it was revealed that low MW was substantially reduced by the activity of microbial communities in the MBR whereas high MW efficiently decreased by the NF membrane. These patterns agreed with that low MW strongly supports microbial growth compared with high MW [27].

The FEEM spectra of standard substances are illustrated in Fig. 3. The Excitation-emission matrix (EEM) intensity was expressed by contour lines. Bovine serum albumin (BSA) (Sigma-Aldrich, St Louis, MO, USA) has a maximum peak at an excitation (Ex) wavelength of 280 nm and an emission (Em) wavelength of 340 nm. The Suwannee River humic acid (SRHA) (IHSS, St. Paul, MN, USA) and the Suwannee River fulvic acid (SRFA) (IHSS, St. Paul, MN, USA) have two pairs of maximum peak locations. SRHA and SRFA showed a maximum peak at Ex = 270 nm/Em = 450 nm and Ex = 320 nm/Em = 440 nm, and at Ex = 260 nm/Em = 440 nm and Ex = 320 nm/Em = 440 nm, respectively. Previous studies proposed that peak of protein-like substances could be found at Ex = 270–280 nm and Em = 320–350 nm, and the peak of humic-like substances could be found at Ex = 250–260 nm, Em = 380–480 nm or Ex = 330–350 nm, Em = 420–480 nm [28]. Changes in fluorescence spectra through the MBR–NF systems were shown in Fig. 4. The distinct protein-like and humic-like fluorescence peaks were found for MBR feed sample but intensities of those were slightly reduced after the MBR process. Furthermore, peaks for both protein- and humic-like substances for MBR effluent sample were completely removed after the NF membrane. The observations correspond to the DOC removal patterns after the MBR and NF membrane processes.

3.2. Characterization of membrane fouling

The differences between characteristics of desorbed membrane foulants from MF in MBR and NF membranes, including foulants characteristics, nitrogen characteristics, and inorganic compositions of floulants, are provided in Table 6. The amount of desorbed membrane foulants with 0.1N NaOH was substantially higher than those of desorbed foulants with 0.1 N HCl. The alkaline solution (i.e., NaOH) was more effective than acid solutions (i.e., HCl) to desorb membrane foulants [29], which means flux of fouled membrane may be more

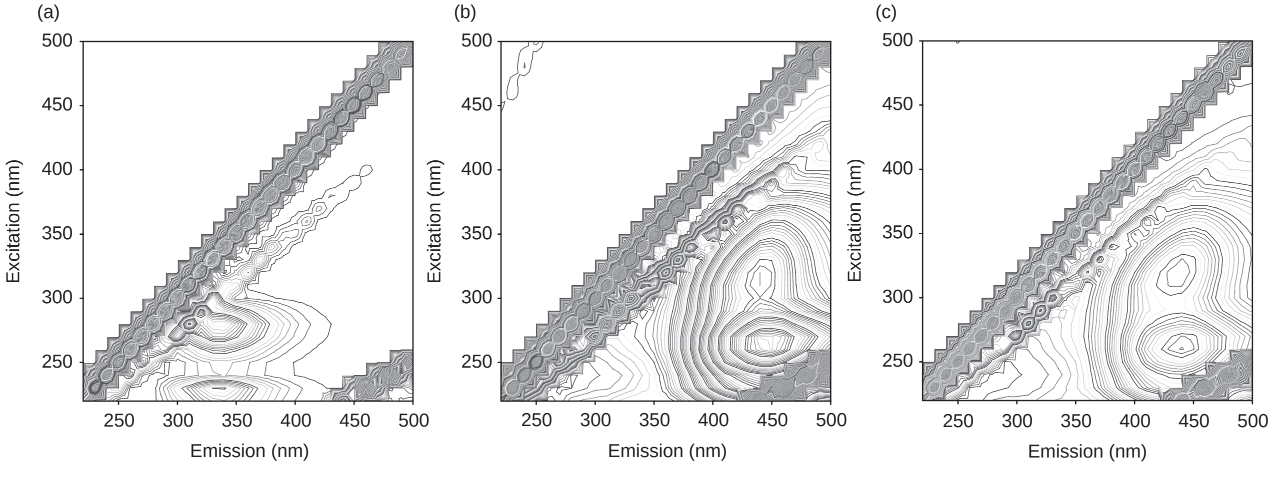

Fig. 3. Fluorescence contour plot of standard substances: (a) BSA, (b) SRHA, and (c) SRFA.

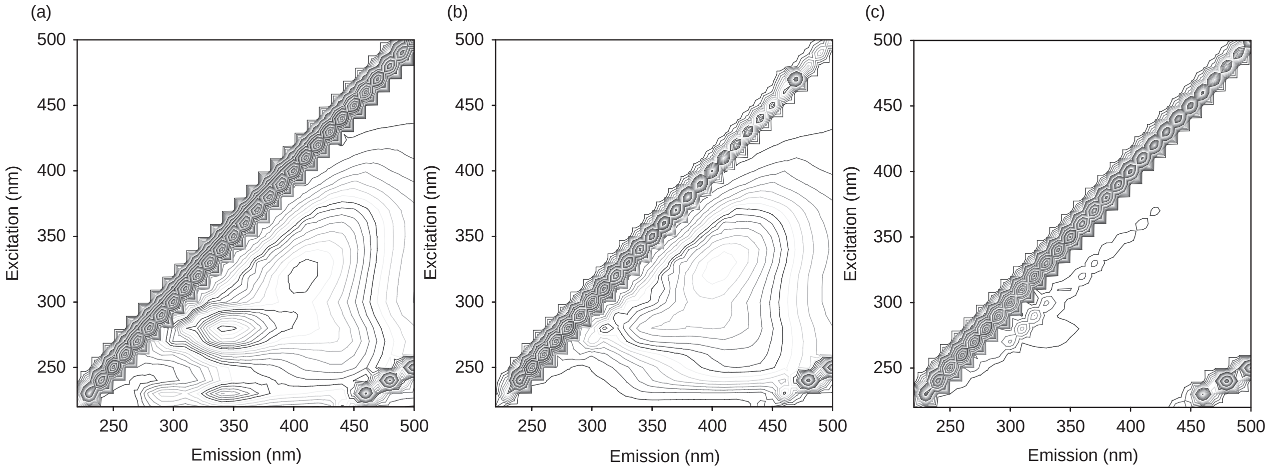

Fig. 4. Contour plots of 3D FEEM from wastewater reclamation system: (a) MBR feed, (b) MBR effluent, and (c) NF effluent.

Table 6
Characteristics of desorbed membrane foulants from MF in MBR and NF membrane.

			MF-base	MF-acid	NF-base	NF-acid
Foulants characteristics	Desorbed DOC (mgC/m^2)		610.5 (±3.5)	10.2 (±0.2)	469.6 (±6.0)	12.2 (±0.7)
	UV_{254} (cm^{-1})		0.227 (±0.000)	0.008 (±0.000)	0.128 (±0.000)	0.003 (±0.000)
	SUVA (L m^{-1} mg^{-1})		1.2 (±0.01)	2.6 (±0.02)	2.3 (±0.03)	2.3 (±0.13)
Nitrogen characteristics	Desorbed TN (mgN/m^2)		100.0 (±0.60)	5.2 (±0.45)	92.1 (±1.09)	9.8 (±0.71)
	Desorbed inorganic nitrogen (mgN/m^2)	Total	17.3 (±0.00)	4.5 (±0.34)	15.0 (±2.00)	9.8 (±0.74)
		Nitrite	ND	ND	ND	ND
		Nitrate	14.3 (±0.18)	2.6 (±0.14)	6.2 (±0.12)	1.4 (±0.33)
		Ammonium	2.9 (±0.18)	1.9 (±0.20)	8.7 (±2.12)	8.4 (±1.07)
	Desorbed org-N (mgN/m^2)		82.9 (±0.72)	1.0 (±0.43)	77.7 (±2.00)	0.2 (±0.10)
	org-N/C (M)		0.116 (±0.002)	0.081 (±0.038)	0.143 (±0.004)	0.013 (±0.007)
Inorganic compositions of foulants	Mg (mg/m^2)		286.7	ND	734.6	393.0
	Ca (mg/m^2)		13234.6	3235.3	13771.5	7838.9
	Al (μg/m^2)		4119.0	923.5	2613.3	1927.1
	As (μg/m^2)		16.4	1.8	55.5	7.7
	Cu (μg/m^2)		1077.6	573.5	25204.7	4527.1
	Fe (μg/m^2)		3365.2	796.1	601.2	267.3
	Mn (μg/m^2)		1265.4	83.4	221.8	198.9
	Si (mg/m^2)		19.4	1.2	62.3	3.4

ND: not detected.

easily recovered by alkaline solutions than acid solutions. In case of nitrogen characteristics, the amounts of organic nitrogen from MF–base (desorbed MF foulants using base solution) and NF–base (desorbed NF foulants using base solution) was higher than those of MF–acid (desorbed MF foulants using acid solution) and NF–acid (desorbed NF foulants using acid solution). Microbial activity is believed to be evaluated with org-N/C molar ratio as organic nitrogen compounds, such as amino acids, are derived from microbial by-products, from either algae or bacteria [16]. The org-N/C was inversely proportional to corresponding SUVA values from desorbed membrane foulants, as described in Fig. 5. From the comparison between inorganic metal compositions of membrane fouling from MF in MBR and NF membranes, it was identified that calcium, aluminum, iron,

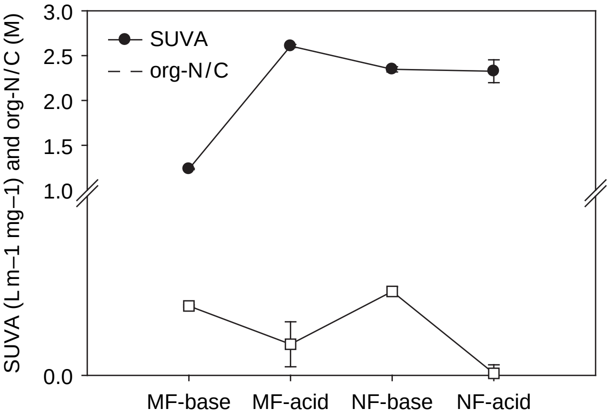

Fig. 5. Comparison of variations between SUVA and org-N/C.

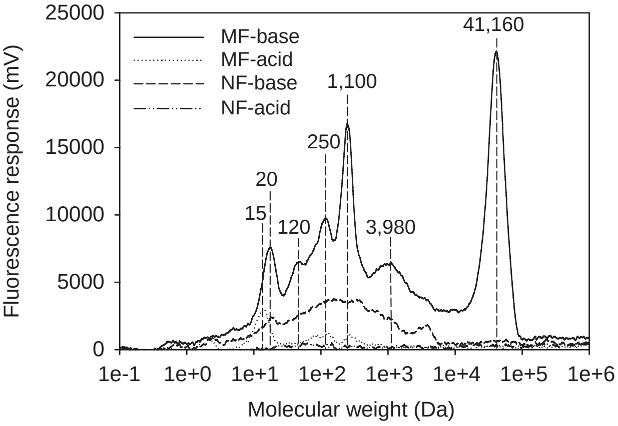

Fig. 7. MW distribution of protein-like substances from MF and NF membrane foulants.

and silicon were dominant species of inorganic materials for membrane foulants.

The MW distribution of aromatic substances from both the MF and NF foulants was compared in Fig. 6. The MW of aromatic substances comprised of both low (510 Da) and high MW (35,410 Da), with highest intensity at 510 Da. Fig. 7 depicts MW distribution of protein-like substances from MF and NF membrane foulants. The MW of protein-like substances ranged from 15 to 41,160 Da. The highest fluorescence response corresponds to a peak at 41,160 Da. Based on MW distribution of those, it was confirmed that the foulants of the MF in MBR and NF membranes were mainly composed of high MW. It indicates that high contents of high MW fractions in feed water infer high fouling potential because membrane fouling desorbed from the MF and NF membrane was primarily composed of hydrophilic fractions.

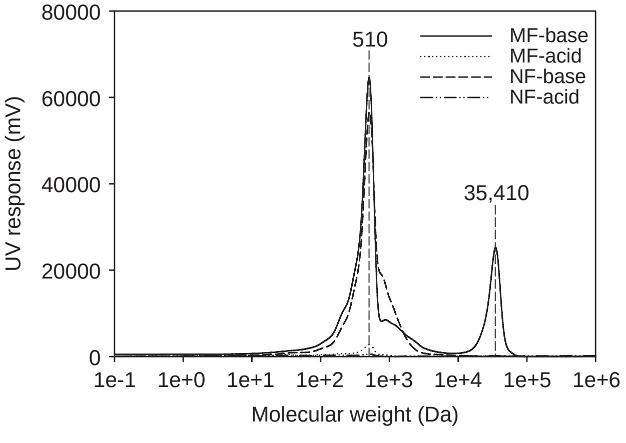

Fig. 6. MW distribution of aromatic substances from MF and NF membrane foulants.

Fluorescence contour maps of MF in MBR and NF membrane foulants are shown in Fig. 8. The MF–base showed two maximum peaks at Ex = 280 nm and Em = 420 nm, Ex =320 nm and Em = 410 nm, and very strong protein-like fluorescence at Ex = 280 nm and Em = 340 nm. However, MF–acid provided two weak maxima at Ex = 310 nm and Em = 410 nm, Ex = 250 nm and Em = 400 nm, and NF–base provided relatively strong two maximum peaks at Ex = 275 nm and Em = 435 nm, Ex = 310 nm and Em = 410 nm compared to MF–acid. In case of NF–acid, its fluorescence intensity was substantially lower than others and represented a very weak peak at Ex = 310 nm and Em = 410 nm, as provided in Table 7. Fig. 9 illustrates excitation–emission matrix of various desorbed foulants. Based on 3D FEEM spectra, it can be considered that the peaks in Group–A correspond to protein-like fluorescence of BSA while most peaks in Group–B were similar to humic-like fluorescence rather than those of protein-like substances. From the fluorescence spectra, it can be postulated that protein-like fraction can strongly contribute to formation of MF membrane foulants in MBR as fluorescence intensity of MF–base was absolutely higher than those of others.

The IR spectra of MF and NF foulants are compared in Fig. 10. The MF (i.e., MF–base and MF–acid) and NF membrane foulants (i.e., NF– base and NF–acid) represented the identical IR peaks. The main functional groups of both MF and NF membrane foulants were amino groups and saccharide groups. The peaks in the region of 3500–3300 cm^{-1} and 850–1125 cm^{-1} were N–H stretching of amides, and the peak in the range of 1680–1630 cm^{-1} was carbonyl group (C=O) of secondary amides [30]. The bacterial cell wall is made of peptidoglycans which were released by cell decomposition. Based on identification

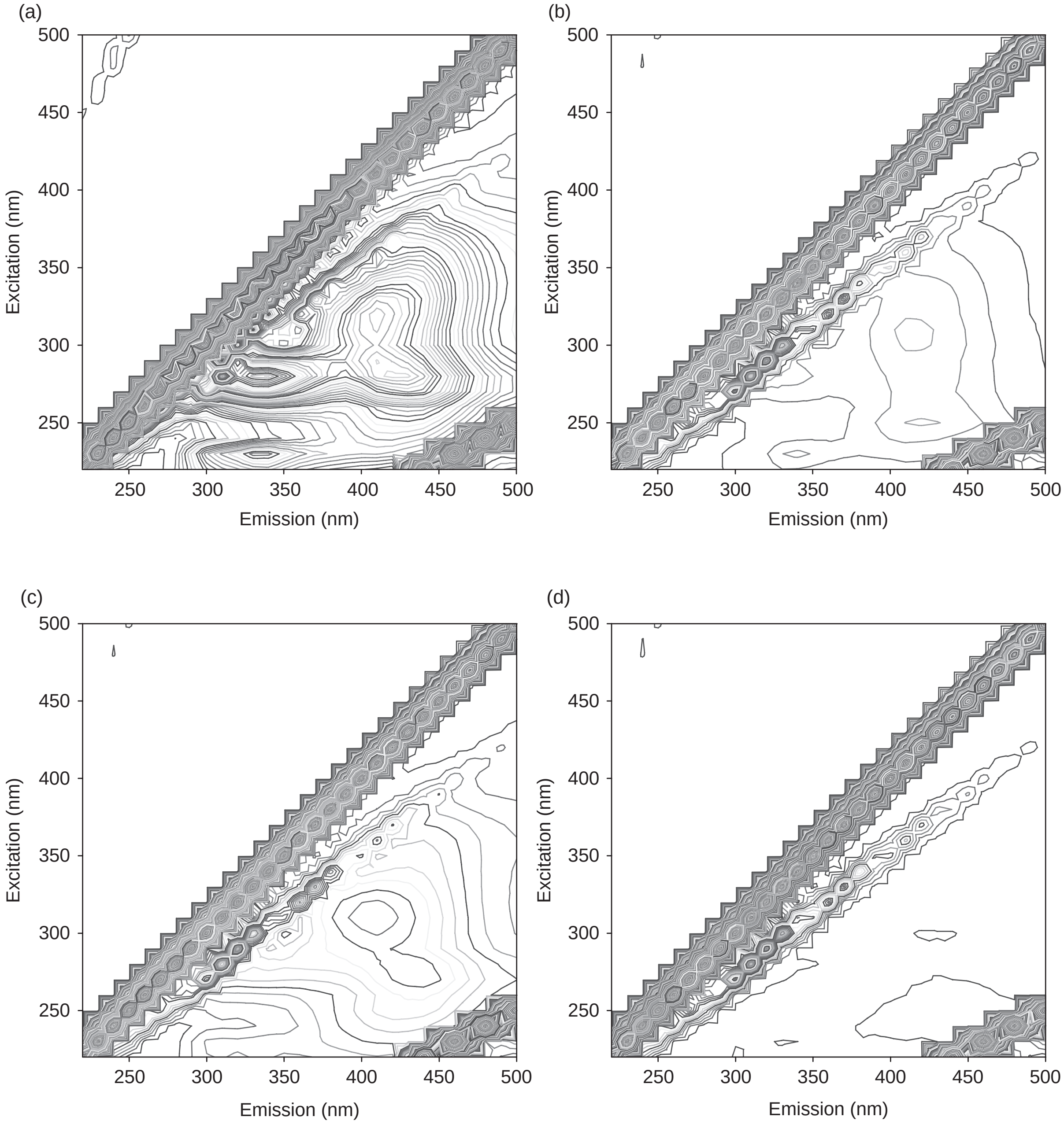

Fig. 8. 3D fluorescence spectra of membrane foulants desorbed from MBR–NF systems: (a) MF–base, (b) MF–acid, (c) NF–base, and (d) NF–acid.

of functional groups in membrane fouling, amino groups may be derived from microorganism by-products in the MBR. The C–O stretching of alcohols usually occurs in the region of 1125–1090 cm^{-1} and 1100–1075 cm^{-1} that were main components of plant cell wall [31]. The O–H stretching of carboxylic acids was appeared in the range of 3100–2900 cm^{-1} and 1440–1395 cm^{-1}, and the peak at 1260 cm^{-1} is indicative of C–O stretching of carboxylic acids which were originated from either aromatic acids or humic substances. The CH band of aldehydes generally occurred in the region of 2800–2900 cm^{-1}. In addition, P–H stretching of phosphorous was appeared in the range of 2440–2275 cm^{-1}. Thus, observations of IR spectra indicate the hydrophilic fractions of organic materials play important roles in foulants formation for the MBR–NF systems.

Table 7
Maximum peak locations and compounds type of the membrane fouling in excitation–emission matrix.

	Maximum peak		Corresponding component
	Excitation (nm)	Emission (nm)	
MF-base	280	340	Protein-like
	280	420	Humic-like
	320	410	Humic-like
MF-acid	310	410	Humic-like
	250	400	Humic-like
NF-base	275	435	Humic-like
	310	410	Humic-like
NF-acid	250	440	Humic-like

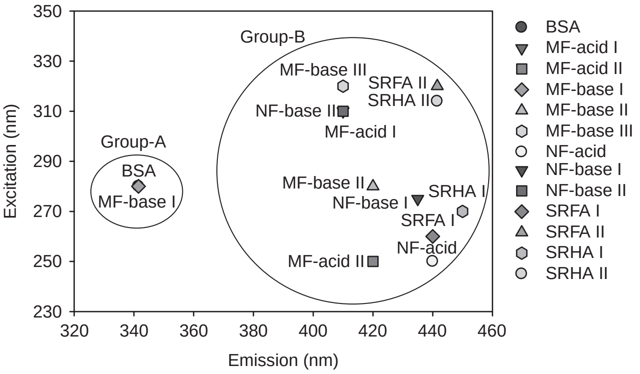

Fig. 9. Excitation–emission matrix of various membrane foulants.

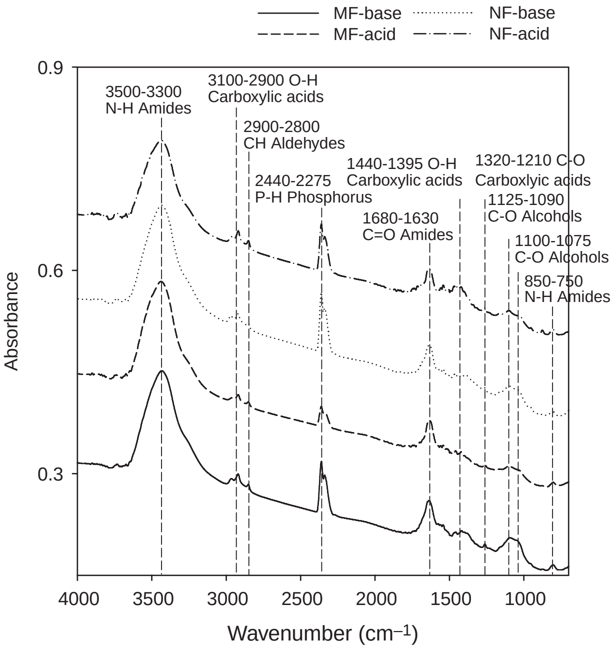

Fig. 10. IR spectra of desorbed membrane foulants.

Table 8
Comparison for structural analyses of membrane foulants desorbed from MF and NF membrane.

	Fractions (%)		
	Hydrophobic fractions	Hydrophilic fractions	Transphilic fractions
MF-base	9	73	19
NF-base	14	80	6

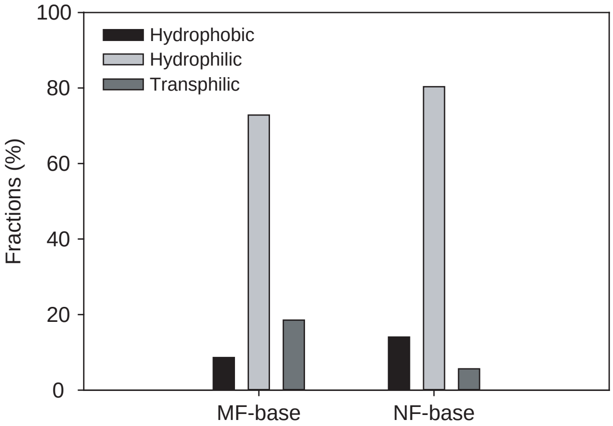

Fig. 11. Fractionatiofins of desorbed membrane foulants by XAD 8/4 resins.

Information of the relative hydrophobicity and hydrophilicity of desorbed foulants was provided in both Table 8 and Fig. 11. The hydrophilic fraction was approximate four times higher than other fractions as foulants in the MF and NF membranes, were mainly comprised of hydrophilic functional groups having O–H and N–H stretching. Many researchers suggested that humic substances play a major role in inevitable formation of membrane fouling [32,33]. However, non-humic substances were found being also responsible for serious membrane fouling in the tested MBR–NF system for wastewater reclamation.

4. Conclusions

MBR–NF systems tested for wastewater reclamation could reduce various contaminants, including organic matters, nitrogen compounds, metals and metalloid, and micropollutants. The hydrophilic fractions of DOC were more efficiently removed than the hydrophobic fractions probably by microorganism activities in MBR. Removal patterns for organic matters could be confirmed by changes in SUVA value, MW distribution, and fluorescence spectra. Nitrogen compounds after nitrification in MBR were substantially reduced through electrostatic interaction with negatively charged NF membrane. NF membrane sufficiently removed almost all the inorganics, except for arsenic. The hydrophilic fractions were major compositions of desorbed membrane foulants for tested MBR–NF systems, which means that non-humic substances (i.e., saccharide and amino groups) might cause significant organic fouling. Rigorous characterization of organic matter and membrane fouling, including HPSEC, fluorescence spectra, IR spectra, and XAD 8/4 resin fractionation, revealed that hydrophilic contents, comprising of protein-like substances (i.e., amide and amine groups) and/or saccharide groups, were responsible for significant membrane fouling in this filtration system for wastewater reclamation.

Acknowledgments

This research was supported by a grant from the National Research Laboratory Program by the Korea Science and Engineering Foundation (NOM laboratory: R0A-2007-000-20055-0).

References

[1] T. Asano, F.L. Burton, H.L. Leverenz, R. Tsuchihashi and G. Tchobanoglous, Water Reuse: Issues, Technologies, and Applications, McGraw Hill, New York, USA, 2007.

[2] P. Côte, H. Buisson, C. Pound and G. Arakaki, Desalination, 113 (1997) 189–196.

[3] P. Côté, M. Masini and D. Mourato, Desalination, 167 (2004) 1–11.

[4] T. Wintgens, T. Melin, A. Schiller, S. Khan, M. Muston, D. Bixio and C. Thoeye, Desalination, 178 (2005) 1–11.

[5] M. Marcucci, G. Nosenzo, G. Capannelli, I. CiabattP, D. Corrieri and G. Ciardelli, Desalination, 138 (2001) 75–82.

[6] C. Merza, R. Scheumanna, B. El Hamouri and M. Kraume, Desalination, 215 (2007) 37–43.

[7] J.H. Choi, S. Dockko, K. Fukushi and K. Yamamoto, Desalination, 146 (2002) 413–420.

[8] J.H. Choi, K. Fukushi and K. Yamamoto, Water Sci. Tech., 51(6–7) (2005) 305–312.

[9] J.H. Choi, K. Fukushi, H.Y. Ng and K. Yamamoto, Water Sci. Tech., 53(6) (2005) 131–136.

[10] A.M. Comerton, R.C. Andrews and D.M. Bagley, Water Res., 39 (2005) 3982–3990.

[11] S.P. Hong, T.H. Bae, T.M Tak, S. Hong and A. Randall, Desalination, 143 (2002) 219–228.

[12] F.I. Hai, K. Yamamoto and K. Fukushi, Desalination, 180 (2005) 89–97.

[13] K.H. Choo and C.H. Lee, Water Res, 30(8) (1996) 1771–1780.

[14] J. Cho, G. Amy, J. Pellegrino and Y. Yoon, Desalination, 118 (1998) 101–108.

[15] J. Cho, G. Amy and J. Pellegrino, Water Res., 33(11) (1999) 2517–2526.

[16] E.M. Thurman, Organic Geochemistry of Natural Waters, M. Nijhoff and W. Junk Publishers, Dordrecht, The Netherlands, 1985.

[17] S. Lee, N. Quyet, E. Lee, S. Kim, S. Lee, Y.D. Jung, S.H. Choi and J. Cho, Desalination, 221 (2008) 234–237.

[18] B.J. Vanderford and S.A. Snyder, Environ. Sci. Technol., 40 (2006) 7312–7320.

[19] N. Her, G. Amy, D. Foss, J. Cho, Y. Yoon and P. Kosenka, Environ. Sci. Technol., 36 (2002) 1069–1076.

[20] B. Kwon, S. Lee, J. Cho, H. Ahn, D. Lee and H.S. Shin, Environ. Sci. Technol., 39 (2005) 732–739.

[21] C.H. Chang and O.J. Hao, J. Chem. Tech. Biotechnol., 67 (1996) 27–38.

[22] D. Said-Pullicino, F.G. Erriquens and G. Gigliotti, Bioresource Technol., 98 (2007) 1822–1831.

[23] X. Zhu and M. Elimelech, Environ. Sci. Technol., 31 (1997) 3654–3662.

[24] A. Seidel, J.J. Waypa and M. Elimelech, Environ. Eng. Sci., 18(2) (2001) 105–113.

[25] S.A. Snyder, P. Westerhoff, Y. Yoon and D.C. Sedlak, Environ. Eng. Sci., 20 (2003) 449–469.

[26] S.A. Snyder, S. Adham, A.M. Redding, F.S. Cannon, J. De Carolis, J. Oppenheimer, E.C. Wert and Y. Yoon, Desalination, 202 (2007) 156–181.

[27] J.L. Meyer, R.T. Edwards, R. Risley, Microb. Ecol., 13 (1987) 13–29.

[28] P.G. Coble, Marine Chem., 51 (1996) 325–346.

[29] H. Yamamura, K. Kimura and Y. Watanabe, Environ. Sci. Technol., 41 (19) (2007) 6789–6794.

[30] D.A. Skoog and J.J. Leary, Principles of Instrumental Analysis, 4th edition, Saunders College Publishing, New York, USA, 1992.

[31] N. Lee, G. Amy and J.P. Croué, Water Res., 40 (2006) 2357–2368.

[32] C. Combe, E. Molis, P. Lucas, R. Riley and M. Clark, J. Memb. Sci., 154 (1999) 73–87.

[33] K. Jones and C. O'Melia, J. Memb. Sci., 165 (2000) 31–46.